JOURNAL OF AIRCRAFT
Vol. 41, No. 6, November–December 2004

Thermal Buckling Suppression of Supersonic Vehicle Surface Panels Using Shape Memory Alloy

Xinyun Guo,* Adam Przekop,† and Chuh Mei‡
Old Dominion University, Norfolk, Virginia, 23529-0247
and
Y. Y. Lee§
City University of Hong Kong, Kowloon, Hong Kong, People's Republic of China

An efficient finite element method for the prediction of critical temperature, postbuckling deflection, and vibration characteristics is presented for traditional composite plates embedded with prestrained shape memory alloy (SMA) wires. The temperature-dependent material properties of SMA and composites and the large deflections are considered in the formulation. An iterative eigensolution is presented to determine the critical temperature, the Newton–Raphson method is employed to obtain postbuckling large deflection, and the eigensolver is used to predict free vibration frequencies about the thermally buckled equilibrium positions. Results show that the critical buckling temperature can be raised high enough and that the postbuckling deflection can be completely suppressed for surface panels of supersonic vehicle applications by the proper selection of SMA volume fraction, prestrain, and alloy composition. Weight savings based on critical temperature in the use of SMA as compared with the traditional composite and titanium plates are demonstrated.

Nomenclature

A_s	=	austenite start temperature
$[A]$, $[B]$, $[D]$	=	in-plane, coupling, and bending stiffness matrices of a laminate
a, b, h	=	length, width, and thickness of a plate
$[K]$, $[M]$	=	system linear stiffness and mass matrices
$[K_L]$, $[K_{NL}]$	=	combined system linear and nonlinear stiffness matrices
$[K_{\tan}]$	=	system tangent stiffness matrix
$\{N\}$, $\{M\}$	=	force and moment resultant vectors
$[N_1]$, $[N_2]$	=	system first- and second-order nonlinear incremental stiffness matrices
$\{P\}$, $\{\Delta P\}$	=	system load and imbalanced load vectors
$[\bar{Q}]$	=	transformed lamina reduced stiffness matrix
T_{ref}	=	reference temperature
v_s, v_m	=	volume fractions of shape memory alloy (SMA) fiber and composite matrix
$\{W\}$	=	system nodal displacement vector
α	=	coefficient of thermal expansion (CTE)
ΔT_{cr}	=	critical buckling temperature
ε_r	=	percentage of prestrain of SMA
$\{\kappa\}$	=	bending curvature vector
λ	=	eigenvalue
σ_r	=	recovery stress of SMA

Subscripts

b	=	bending
i	=	iteration number
k	=	layer number of laminates
m	=	membrane or composite matrix
NB, Nm, $N\Delta T$	=	due to $\{N_b\}$, $\{N_m\}$, and $\{N_{\Delta T}\}$, respectively
r	=	due to recovery stress of SMA
s	=	static or a quantity related to SMA
st	=	dependent on both static and dynamic quantities
t	=	dynamic or time dependent
x, y, z	=	plate Cartesian coordinates
ΔT	=	thermal

Introduction

BECAUSE of aerodynamic heating, surface skin panels of supersonic vehicles are subjected to temperatures that can reach several hundred degrees. For example, the skin panel temperature could reach up to 350°F (177°C) for the quiet supersonic platform[1] (QSP) cruising at Mach 2.2–2.4. Large thermal deflections of the skin panels may occur and, thus, result in a poor flight performance. To reduce the large thermal deflections for the X-33, a rugged superalloy thermal protection system (TPS) panel with overlapping seals has been developed. The titanium honeycomb sandwich TPS was designed to be rather stiff, to keep the thermal deflection to a minimum. However, the thin overlapping inconel seals will exhibit flutter and thermal deformation.[2] At present, traditional graphite composite is the candidate for skin panels of QSP proposed by Northrop Grumman.[1]

Shape memory alloys (SMA) have a unique ability to recover large prestrain (up to 8∼10% elongation) completely when the alloy is heated (by the aerodynamic heating) above the austenite finish temperature A_f. The transformation austenite start temperature A_s for Nitinol can be set anywhere between −60°F (−50°C) and +340°F (+170°C) by variation of the nickel content.[3] During the recovery process, a large recovery tensile stress occurs if the SMA wire is restrained. The recovery stress at various prestrain values and the elastic modulus for Nitinol as tested are shown in Figs. 1 and 2 (Ref. 4). An innovative concept is to utilize this large recovery stress by embedding the prestrained SMA wire in a traditional fiber-reinforced laminated composite panel. The SMA wires are, thus, restrained, and large in-plane forces are induced in the panel at temperatures higher than A_s. This stiffening behavior has been experimentally demonstrated with SMA composite beams.[5–7] A comprehensive review of the literature on SMA and its various applications was given by Birman.[8]

Received 7 October 2003; revision received 1 December 2003; accepted for publication 2 December 2003.

*Graduate Research Assistant, Department of Aerospace Engineering. Student Member AIAA.
†Staff Scientist, Department of Aerospace Engineering. Member AIAA.
‡Professor, Department of Aerospace Engineering. Associate Fellow AIAA.
§Assistant Professor, Department of Building and Construction.

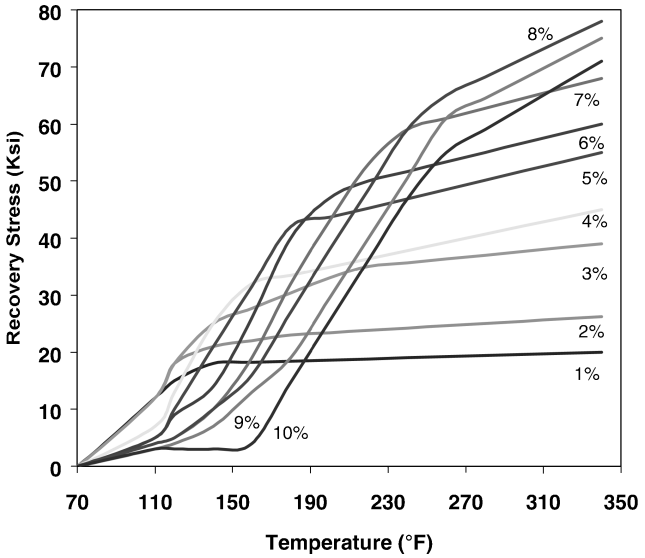

Fig. 1 Nitinol recovery stress at different prestrain.[4]

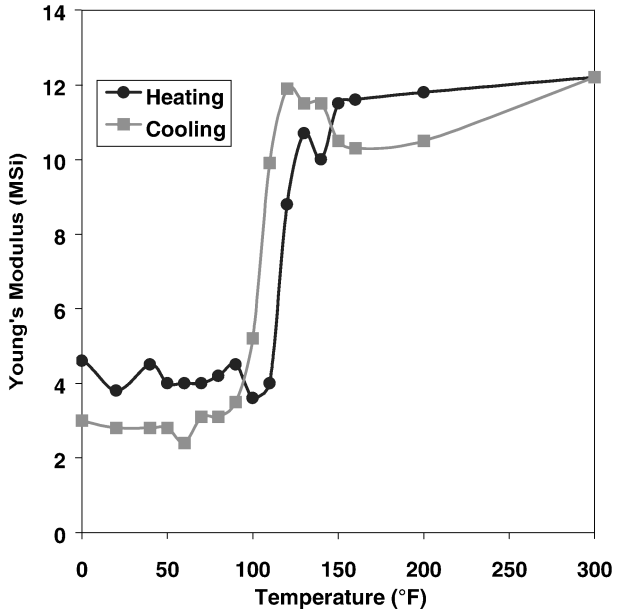

Fig. 2 Nitinol modulus of elasticity.[4]

Effects of temperature-dependent (TD) material properties on buckling of plate and shell structures have been summarized in three excellent review papers.[9–11] Kamiya and Fukui[12] investigated the postbuckling of square isotropic plates with TD properties. The finite difference method with an iteration scheme was used, and they obtained results for plates of simply supported and clamped edges with constrained in-plane displacements. They found that the TD properties lead to a lower critical temperature and reduce the postbuckling stiffness because the properties of common materials tend to deteriorate at high temperatures. Chen and Chen[13,14] proposed a finite element method (FEM) for thermal buckling behavior of laminated composite plates. The TD properties lower predictions of critical temperature and reduce thermal postbuckling strength. Noor and Burton[15] studied the effects of TD properties on the prebuckling stresses, critical temperatures, and their sensitivity derivatives of antisymmetric angle-ply plates using the three-dimensional thermoelasticity solutions. Numerical results show that the TD properties reduce critical temperatures, and the influence of prebuckling stresses on critical temperature is less significant for the TD than the temperature-independent (TI) property case. Lee et al.[16] studied the thermal effect for stiffened composite plates with the material degradation on the buckling, vibration, and flutter characteristics using FEM. Their results indicate that the material degradation decreases the critical temperature and increases the postbuckling deflection. Note that the TD material properties were all assumed in linear functions of temperature in the preceding references.[12–16]

For the highly nonlinear TD properties of Nitinol shown in Figs. 1 and 2, Mei et al.[17] proposed an iterative eigenvalue method for determination of the critical temperature ΔT_{cr} of SMA embedded composite laminates. Duan,[18] Duan et al.,[19] and Tawfik et al.[20] developed an incremental-updated Lagrangian FEM (IUL/FEM) for the analysis of thermal buckling of SMA embedded composite plate. The temperature range interested is divided into many small increments. For each small temperature increment, the averaged material properties were approximated as constant. The initial displacement and initial stresses were considered in the formulation. The marching method in temperature is used to determine the thermal deflections and stresses for each temperature. The drawback of this method is the high cost of computational time due to many small temperature increments.

Lee and Choi[21] and Lee et al.[22] studied the thermal buckling and postbuckling of composite beams and shells with embedded SMA actuators, respectively. Based on the one-dimensional thermomechanical constitutive equation of SMA wire actuators, a simple formula was suggested to calculate the critical buckling temperature of a beam once the SMA actuator is activated.[21] This constitutive equation of SMA was also incorporated into a finite element model as an ABAQUS subroutine to determine the thermal postbuckling lateral deflections of the beam,[21] plate, and shell.[22] The results showed an increased critical buckling temperature and reduced lateral deflection. They also found that the austenite start temperature is significant in determining the critical temperature. However, the recovery stresses calculated from the theoretical constitutive equation were much different from the experimental data. Thompson and Loughlan[23] manufactured and experimented with SMA wire embedded laminated panels, as well as carrying out a numerical finite element analysis using MSC/NASTRAN. The manufacturing methodology of the hybrid SMA carbon/epoxy panel is described in detail. The panel was embedded with 23 0.3-mm- (0.012-in.-)-diameter SMA actuators with an initial prestrain 6%. Both experiment and numerical analysis showed that the out-of-plane displacement of the postbuckled laminated panel could be reduced by utilization of the induced recovery forces from SMA actuators.

This paper presents an improved and efficient FEM for thermal buckling of plates with nonlinear TD material properties. The approach is based on thermal strain being a cumulative physical quantity, whereas the stress is an instant one. Thus, the thermal strain is an integral quantity of thermal expansion coefficient with respect to temperature,[24] whereas stress is evaluated with the instant elastic modulus at certain temperature in the thermoelastic stress–strain relations.[7] Therefore, the method does not need the many small increments as in the marching method,[18–20] and it is suitable for any nonlinear TD material properties naturally considered in the integral formulation of the calculation of thermal strain. The iterative eigensolution method[17] is employed to determine ΔT_{cr}, and the Newton–Raphson iteration method is used to obtain postbuckling deflection. This approach substantially reduces computational time as compared with the IUL/FEM method. Advanced thermoplastics such as polythereterketone (PEEK), polyphenylee sulfide (PPS), etc., are now used in the temperature range up to 600–700°F (315–370°C). In the present paper, graphite–epoxy composite panels with or without SMA embedding are investigated and compared with titanium panels. The use of graphite–epoxy in this paper is only for demonstration of the advantages of SMA in suppression of thermal buckling deflections. Results show that for composite panels embedded with SMA, the critical buckling temperature can be raised high enough and the postbuckling deflection can be suppressed by the proper selection of SMA volume fraction and prestrain for QSP application. The savings in weight based on critical temperature in the use of SMA are also demonstrated.

Finite Element Formulation

Constitutive Thermoelastic Equations

The thermoelastic stress–strain relation for a kth layer of thin SMA embedded composite lamina can be derived and

expressed as[7]

$$\{\sigma\}_k = \begin{Bmatrix}\sigma_x\\ \sigma_y\\ \tau_{xy}\end{Bmatrix}_k$$

$$= [\bar{Q}]_k\left(\{\varepsilon\} - \int_{T_{\text{ref}}}^{T}\{\alpha(\tau)\}_k\,\mathrm{d}\tau\right), \qquad T < A_s$$

$$= [\bar{Q}]_k\{\varepsilon\} + \{\sigma_r\}_k v_{sk} - ([\bar{Q}]_m v_m)_k\int_{T_{\text{ref}}}^{T}(\{\alpha(\tau)\}_m)_k\,\mathrm{d}\tau$$

$$T \geq A_s \quad (1)$$

where $\{\sigma\}$, $\{\alpha\}$, and $\{\sigma_r\}$ denote the stress, thermal expansion coefficient, and SMA recovery stress vectors, respectively; v_s and v_m are the volume fractions of SMA and matrix (graphite–epoxy), respectively; and $[\bar{Q}]$ and $[\bar{Q}]_m$ are the transformed reduced stiffness matrices of the SMA embedded lamina ($v_s \neq 0$) and the matrix ($v_s = 0$). Note that nonlinear thermal strain is inherently cumulative and, thus, an integral is employed. Equation (1) indicates that the SMA embedded composite lamina behaves as a regular one before the SMA is activated, that is, at $T < A_s$; an extra stress term is added to account for the recovery stress after SMA is activated, that is, at $T \geq A_s$. Note that the stiffness matrices $[\bar{Q}]$ and $[\bar{Q}]_m$ are also functions of temperature to account for the TD properties of the graphite–epoxy matrix.

It is assumed that the panel is thin, that is, the ratio of length or width over thickness is greater than 50. The rotary inertia and transverse shear deformation effects are, thus, negligible. The in-plane strains and curvatures, based on von Kármán large deflection and classical laminated plate theories, are given by

$$\{\varepsilon\} = \begin{Bmatrix}u_{,x}\\ v_{,y}\\ u_{,y}+v_{,x}\end{Bmatrix} + \frac{1}{2}\begin{Bmatrix}w_{,x}^2\\ w_{,y}^2\\ 2w_{,x}\,w_{,y}\end{Bmatrix} + z\begin{Bmatrix}-w_{,xx}\\ -w_{,yy}\\ -2w_{,xy}\end{Bmatrix}$$

$$= \left\{\varepsilon_m^0\right\} + \left\{\varepsilon_b^0\right\} + z\{\kappa\} = \{\varepsilon^0\} + z\{\kappa\} \quad (2)$$

where the superscript 0 denotes the midsurface and the subscripts m and b denote membrane (in-plane) and bending components, respectively. The stress resultants per unit length of the SMA embedded composite plate are, thus,

$$\begin{Bmatrix}N\\ M\end{Bmatrix} = \begin{bmatrix}A & B\\ B & D\end{bmatrix}\begin{Bmatrix}\varepsilon^o\\ \kappa\end{Bmatrix} + \begin{Bmatrix}N_r\\ M_r\end{Bmatrix} - \begin{Bmatrix}N_{\Delta T}\\ M_{\Delta T}\end{Bmatrix} \quad (3)$$

where the laminate stiffness matrices and stress resultants are

$$([A],[B],[D]) = \int_{-h/2}^{h/2}[\bar{Q}]_k(1,z,z^2)\,\mathrm{d}z \quad (4)$$

$$(\{N\},\{M\}) = \int_{-h/2}^{h/2}\{\sigma\}_k(1,z)\,\mathrm{d}z \quad (5)$$

$$(\{N_r\},\{M_r\}) = 0, \qquad T < A_s$$

$$= \int_{-h/2}^{h/2}\{\sigma_r\}_k v_{sk}(1,z)\,\mathrm{d}z, \qquad T \geq A_s \quad (6)$$

$$(\{N_{\Delta T}\},\{M_{\Delta T}\}) = \int_{-h/2}^{h/2}\left[[\bar{Q}]_k\int_{T_{\text{ref}}}^{T}\{\alpha(\tau)\}_k\,\mathrm{d}\tau\right](1,z)\,\mathrm{d}z \qquad T < A_s$$

$$= \int_{-h/2}^{h/2}\left[([\bar{Q}]_m v_m)_k\int_{T_{\text{ref}}}^{T}(\{\alpha(\tau)\}_m)_k\,\mathrm{d}\tau\right](1,z)\,\mathrm{d}z \qquad T \geq A_s \quad (7)$$

Equation of Motion

With the application of the variational principle and the kinematic boundary conditions, the governing equation for an SMA embedded composite plate undergoing large deflection subjected to a temperature increase $\Delta T = T - T_{\text{ref}}$ can be written as

$$\begin{bmatrix}M_b & 0\\ 0 & M_m\end{bmatrix}\begin{Bmatrix}\ddot{W}_b\\ \ddot{W}_m\end{Bmatrix} + \left(\begin{bmatrix}K_b & K_{bm}\\ K_{mb} & K_m\end{bmatrix} - \begin{bmatrix}K_{N\Delta T} & 0\\ 0 & 0\end{bmatrix} + \begin{bmatrix}K_r & 0\\ 0 & 0\end{bmatrix}\right.$$

$$+\frac{1}{2}\begin{bmatrix}N_{1Nm}(W_m)+N_{1NB}(W_b) & N_{1bm}(W_b)\\ N_{1mb}(W_b) & 0\end{bmatrix}$$

$$\left.+\frac{1}{3}\begin{bmatrix}N_{2b}\left(W_b^2\right) & 0\\ 0 & 0\end{bmatrix}\right)\begin{Bmatrix}W_b\\ W_m\end{Bmatrix} = \begin{Bmatrix}P_{b\Delta T}\\ P_{m\Delta T}\end{Bmatrix} - \begin{Bmatrix}P_{br}\\ P_{mr}\end{Bmatrix} \quad (8)$$

or, simply,

$$[M]\{\ddot{W}\} + \left([K] - [K_{N\Delta T}] + [K_r] + \tfrac{1}{2}[N_1(W)]\right.$$

$$\left. + \tfrac{1}{3}[N_2(W^2)]\right)\{W\} = \{P_{\Delta T}\} - \{P_r\} \quad (9)$$

where $[M]$ and $[K]$ are the system mass and linear stiffness matrices; the geometrical stiffness matrices $[K_{N\Delta T}]$ and $[K_r]$ are due to thermal in-plane force $\{N_{\Delta T}\}$ and SMA recovery in-plane force $\{N_r\}$, respectively; and $[N_1]$ and $[N_2]$ are the first and second-order incremental stiffness matrices that depend linearly and quadratically on system displacement vector $\{W\}$, respectively. System load vectors $\{P_{\Delta T}\}$ and $\{P_r\}$ are due to thermal and SMA recovery stress resultants, respectively. The subscripts b and m denote bending and in-plane components, respectively; subscripts mb (bm), Nm, and NB indicate that the corresponding stiffness matrices are dependent on laminate coupling stiffness $[B]$, in-plane force components $\{N_m\} = ([A]\{\varepsilon_m^o\})$, and $\{N_B\} = ([B]\{\kappa\})$, respectively.

Solution Procedure

Critical Buckling Temperature

For a plate to have a nonzero critical buckling temperature the following criteria must be met: 1) The laminate must be symmetric, that is, $[B] = 0$, thus, $[K_{bm}] = [K_{mb}] = [N_{1NB}] = 0$. 2) Out-of-plane forces should be zero, that is, $\{P_{b\Delta T}\} = \{P_{br}\} = 0$. The dynamic term $[M]\{\ddot{W}\}$ is also neglected for this static problem. Therefore, Eq. (8) reduces to

$$\left(\begin{bmatrix}K_b & 0\\ 0 & K_m\end{bmatrix} - \begin{bmatrix}K_{N\Delta T} & 0\\ 0 & 0\end{bmatrix} + \begin{bmatrix}K_r & 0\\ 0 & 0\end{bmatrix} + \frac{1}{2}\begin{bmatrix}N_{1Nm} & N_{1bm}\\ N_{1mb} & 0\end{bmatrix}\right.$$

$$\left. + \frac{1}{3}\begin{bmatrix}N_{2b} & 0\\ 0 & 0\end{bmatrix}\right)\begin{Bmatrix}W_b\\ W_m\end{Bmatrix} = \begin{Bmatrix}0\\ P_{m\Delta T}\end{Bmatrix} - \begin{Bmatrix}0\\ P_{mr}\end{Bmatrix} \quad (10)$$

From the second equation of Eq. (10), the in-plane displacement $\{W_m\}$ can be expressed in terms of bending displacement $\{W_b\}$ as

$$\{W_m\} = [K_m]^{-1}(\{P_{m\Delta T}\} - \{P_{mr}\}) - \tfrac{1}{2}[K_m]^{-1}[N_{1mb}]\{W_b\}$$

$$= \{W_m\}_0 - \{W_m\}_2 \quad (11)$$

where $\{W_m\}_0$ is a constant vector, and $\{W_m\}_2$ is quadratically dependent on $\{W_b\}$. Thus, the matrix $[N_{1Nm}(\{W_m\})]$ is the algebraic sum of two matrices: $[N_{1Nm}(\{W_m\}_0)]$ and $[N_{1Nm}(\{W_m\}_2)]$. For clarity, $[N_{1Nm}(\{W_m\}_0)]$ is denoted as $[N_{0Nm}]$ and $[N_{1Nm}(\{W_m\}_2)]$ as $[N_{2Nm}]$.

Therefore, the first equation of Eq. (10) is expressed in terms of the bending displacement $\{W_b\}$ only as

$$\left([K_L] + \left[K_{NL}\left(W_b^2\right)\right]\right)\{W_b\} = \{0\} \quad (12)$$

where the combined linear and cubic nonlinear stiffness matrices are given by

$$[K_L]\{W_b\} = \big([K_b] - [K_{N\Delta T}] + [K_r] + \tfrac{1}{2}[N_{0Nm}]\big)\{W_b\} + \tfrac{1}{2}[N_{1bm}(\{W_b\})]\{W_m\}_0 = ([K_b] - [K_{N\Delta T}] + [K_r] + [N_{0Nm}])\{W_b\} \quad (13)$$

$$\big[K_{NL}\big(W_b^2\big)\big]\{W_b\} = \big[\tfrac{1}{3}[N_{2b}] - \tfrac{1}{2}[N_{2Nm}] - \tfrac{1}{4}[N_{1bm}][K_m]^{-1}[N_{1mb}]\big]\{W_b\} \quad (14)$$

The linear term $[K_L]\{W_b\}$ is reached due to the relation that[18] $[N_{1Nm}(\{W_m\}_0)]\{W_b\} = [N_{1bm}]\{W_m\}_0$. The nonlinear stiffness $[K_{NL}]$ does not exist for linear eigenvalue problem in the determination of $\Delta T_{\rm cr}$. The linear stiffness $[K_L]$ can be divided into two groups: the matrices $[K_{N\Delta T}(\Delta T)]$, $[K_r(\Delta T)]$, and $[N_{0Nm}(\Delta T)]$ are function of temperature increase, and the matrix $[K_b]$ is not. Under the assumption that $\Delta T_{\rm cr} = \lambda \Delta T$, Eq. (12) can be transformed into an eigenvalue problem as

$$[K_b]\{\Delta W_b\} = ([K_{N\Delta T}(\lambda\Delta T)] - [K_r(\lambda\Delta T)] - [N_{0Nm}(\lambda\Delta T)])\{\Delta W_b\} \quad (15)$$

If $[K_{N\Delta T}]$, $[K_r]$, and $[N_{0Nm}]$ are all linear functions of temperature, Eq. (15) becomes

$$[K_b]\{\Delta W_b\} = \lambda([K_{N\Delta T}(\Delta T)] - [K_r(\Delta T)] - [N_{0Nm}(\Delta T)])\{\Delta W_b\} \quad (16)$$

and the critical temperature for a panel with TI material properties is determined as

$$\Delta T_{\rm cr} = \lambda_1 \Delta T \quad (17)$$

where λ_1 is the lowest eigenvalue. However, $[K_r]$ is due to SMA recovery in-plane force $\{N_r\}$, which is a highly nonlinear function of temperature. The iterative scheme proposed by Mei et al.[17] is employed here. An initial trial ΔT is given, and the eigenvalues of Eq. (15) are calculated. Then the lowest eigenvalue λ_1 is used to update ΔT, for the ith iteration. ΔT is updated by

$$\Delta T_{i+1} = (\lambda_1)_i \Delta T_i \quad (18)$$

All of the stiffness matrices $[K_{N\Delta T}]$, $[K_r]$, and $[N_{0Nm}]$ are updated with ΔT_{i+1}. The critical buckling temperature is reached when λ_1 is close to 1 ($|\lambda_1 - 1| \le 0.001$ in this paper). It is possible that if the parameters or the SMA is not activated in certain circumstances, there might exist an early buckling region. In this case, the SMA embedded would have two critical buckling temperatures.[7] Therefore, a better way to determine the critical buckling temperature is through the investigation of postbuckling deflections as described hereafter.

Thermal Postbuckling Deflections

For static thermal problem, the system equation from Eq. (8) is a set of nonlinear algebraic equations as

$$\left(\begin{bmatrix} K_b & K_{bm} \\ K_{mb} & K_m \end{bmatrix} - \begin{bmatrix} K_{N\Delta T} & 0 \\ 0 & 0 \end{bmatrix} + \begin{bmatrix} K_r & 0 \\ 0 & 0 \end{bmatrix} + \frac{1}{2}\begin{bmatrix} N_{1Nm} + N_{1NB} & N_{1bm} \\ N_{1mb} & 0 \end{bmatrix} + \frac{1}{3}\begin{bmatrix} N_{2b} & 0 \\ 0 & 0 \end{bmatrix}\right)\begin{Bmatrix} W_b \\ W_m \end{Bmatrix} = \begin{Bmatrix} P_{b\Delta T} \\ P_{m\Delta T} \end{Bmatrix} - \begin{Bmatrix} P_{br} \\ P_{mr} \end{Bmatrix} \quad (19)$$

or, simply,

$$\big([K] - [K_{N\Delta T}] + [K_r] + \tfrac{1}{2}[N_1] + \tfrac{1}{3}[N_2]\big)\{W\} = \{P_{\Delta T}\} - \{P_r\} \quad (20)$$

the Newton–Raphson iteration method is employed to determine the postbuckling deflection. It is applicable to both symmetrical ($\Delta T > \Delta T_{\rm cr}$) and unsymmetrical (any ΔT) composite laminates. For the ith iteration, the incremental deflection $\{\Delta W\}$ is related to the imbalanced load $\{\Delta P\}$ by the tangent stiffness as

$$[K_{\tan}]_i\{\Delta W\}_{i+1} = \{\Delta P\}_i \quad (21)$$

where the tangent stiffness and the imbalance load vector are[18]

$$[K_{\tan}]_i = [K] - [K_{N\Delta T}] + [K_r] + [N_1]_i + [N_2]_i \quad (22)$$

$$\{\Delta P\}_i = \{P_{\Delta T}\} - \{P_r\} - \big([K] - [K_{N\Delta T}] + [K_r] + \tfrac{1}{2}[N_1]_i + \tfrac{1}{3}[N_2]_i\big)\{W\}_i \quad (23)$$

The subscript i to the nonlinear incremental stiffness matrices in Eqs. (22) and (23) denotes that they are evaluated with $\{W\}_i$. The incremental displacement vector $\{\Delta W\}_{i+1}$ can be calculated from Eq. (21). Then the displacement vector $\{W\}$ is updated as

$$\{W\}_{i+1} = \{W\}_i + \{\Delta W\}_{i+1} \quad (24)$$

The solution procedure seeks to reduce the imbalanced force vector $\{\Delta P\}$ and, consequently, $\{\Delta W\}$, to a specified small quantity. In this study, the absolute value of the maximum component of $|\{\Delta W\}|$ is set to less than 1% of the shell thickness.

Vibration of Thermally Buckled Composite Plates

Once the static thermal postbuckling deflection is obtained for a certain rise of temperature ΔT, the linear vibration frequencies of the thermally buckled plate about this buckled equilibrium position can be determined. Mathematically, the solution of a differential equation with steady-state forcing terms can be considered as the summation of a time-independent particular solution and a TD homogenous solution, as follows:

$$\{W\} = \{W\}_s + \{W(t)\}_t \quad (25)$$

Physically, $\{W\}$ is the total displacement, $\{W\}_s$ is the TI static solution that refers to the thermal postbuckling deflection, and $\{W(t)\}_t$ is the TD homogenous solution that refers to the dynamic vibration.

Substitution of Eq. (25) into the system equation Eq. (9) leads to

$$[M](\{\ddot{W}\}_s + \{\ddot{W}\}_t) + \big([K] - [K_{N\Delta T}] + [K_r] + \tfrac{1}{2}[N_1]_{s+t} + \tfrac{1}{3}[N_2]_{s+t}\big)(\{W\}_s + \{W\}_t) = \{P_{\Delta T}\} - \{P_r\} \quad (26)$$

where subscript $s+t$ denotes that the corresponding nonlinear stiffness matrix is evaluated by the sum of $\{W\}_s$ and $\{W\}_t$.

The matrix $[N_1]_{s+t}$ is the combination of the first-order nonlinear stiffness matrices, which are linearly dependent on $\{W\}$. The evaluation can be expressed as

$$[N_1]_{s+t} = [N_1]_s + [N_1]_t \quad (27)$$

where the subscripts s and t denote that the corresponding matrix is evaluated by $\{W\}_s$ or $\{W\}_t$, respectively. The matrix $[N_2]_{s+t}$ is a second-order nonlinear stiffness matrix that is quadratically dependent on $\{W\}$. Thus, there exists a term $[N_2]_{st}$ due to the coupling or that is a product of $\{W\}_s$ and $\{W\}_t$. The matrix $[N_2]_{s+t}$ can be expressed as

$$[N_2]_{s+t} = [N_2]_s + [N_2]_t + 2[N_2]_{st} \quad (28)$$

By substitution of Eqs. (27) and (28) into Eq. (26), recognition that the time derivatives of $\{W\}_s$ are zero, and the collection of static terms (including static loadings) and dynamic terms separately, the system equation of motion can be grouped into two equations as

$$\big([K] - [K_{N\Delta T}] + [K_r] + \tfrac{1}{2}[N_1]_s + \tfrac{1}{3}[N_2]_s\big)\{W\}_s = \{P_{\Delta T}\} - \{P_r\} \quad (29)$$

Table 1 Material properties of Nitinol, graphite–epoxy composite lamina and titanium

Nitinol	Graphite–Epoxy	Titanium
See Figs. 1 and 2 for Young's modulus and recovery stresses	E_1 22.5 × 10^6 $(1-3.53\times10^{-4}\cdot\Delta T)$ psi [155 $(1-6.35\times10^{-4}\cdot\Delta T)$ GPa]	E 14.94 × 10^6 psi (103 GPa)
G, 3.604 × 10^6 psi, $T < A_s$ (24.9 GPa)	E_2 1.17 × 10^6 $(1-4.27\times10^{-4}\cdot\Delta T)$ psi [8.07 $(1-7.69\times10^{-4}\cdot\Delta T)$ GPa]	ρ 0.424 × 10^{-3} lb · s^2/in.^{4} (4510 kg/m^3)
3.712 × 10^6 psi, $T \geq A_s$ (25.6 GPa)	G_{12} 0.66 × 10^6 $(1-6.06\times10^{-4}\cdot\Delta T)$ psi [4.55 $(1-1.09\times10^{-3}\cdot\Delta T)$ GPa]	μ 0.37
ρ 0.6067 × 10^{-3} lb · s^2/in.^{4} (6450 kg/m^3)	ρ 0.1458 × 10^{-3} lb · s^2/in.^{4} (1550 kg/m^3)	α 4.78 × 10^{-6}/°F (8.6 × 10^{-6}/°C)
μ 0.3	μ_{12} 0.22	
α 5.7 × 10^{-6}/°F (10.26 × 10^{-6}/°C)	α_1 $-0.04\times10^{-6}(1-1.25\times10^{-3}\cdot\Delta T)$/°F [$-0.07\times10^{-6}(1-0.69\times10^{-3}\cdot\Delta T)$/°C]	
	α_2 16.7 × $10^{-6}(1+0.41\times10^{-4}\cdot\Delta T)$/°F [30.6 × $10^{-6}(1+0.28\times10^{-4}\cdot\Delta T)$/°C]	

$$[M]\{\ddot{W}\}_t + \left([K] - [K_{N\Delta T}] + [K_r] + \tfrac{1}{2}[N_1]_t + \tfrac{1}{3}[N_2]_t\right)\{W\}_t + \left(\tfrac{1}{2}[N_1]_t + \tfrac{1}{3}[N_2]_t + \tfrac{2}{3}[N_2]_{st}\right)\{W\}_s + \left(\tfrac{1}{2}[N_1]_s + \tfrac{1}{3}[N_2]_s + \tfrac{2}{3}[N_2]_{st}\right)\{W\}_t = 0 \quad (30)$$

Note that Eq. (29) is identical to Eq. (20), which is the equation for static postbuckling deflection $\{W\}_s$ ($\{W\}_s = \{W\}$ in Eq. (20) because $\{W\}_t = 0$ for pure static problems).

The following transformations hold by examination of the element level definitions[18]:

$$[N_1]_t\{W\}_s = [N_1]_s\{W\}_t \quad (31)$$

$$[N_2]_t\{W\}_s = [N_2]_{st}\{W\}_t \quad (32)$$

$$[N_2]_{st}\{W\}_s = [N_2]_s\{W\}_t \quad (33)$$

By substitution of Eqs. (31–33) into Eq. (30), Eq. (30) becomes

$$[M]\{\ddot{W}\}_t + \left([K] - [K_{N\Delta T}] + [K_r] + \tfrac{1}{2}[N_1]_t + \tfrac{1}{3}[N_2]_t\right)\{W\}_t + ([N_1]_s + [N_2]_s + [N_2]_{st})\{W\}_t = 0 \quad (34)$$

Equation (34) represents large-amplitude free vibration about the thermally buckled equilibrium position $\{W\}_s$, which is solved from Eq. (29) or Eq. (20). Once $\{W\}_s$ is known, the matrices $[N1]_s$ and $[N2]_s$ are evaluated with $\{W\}_s$ and, thus, become constant linear stiffness matrices in Eq. (34). Therefore, Eq. (34) can be rearranged by separation of linear and nonlinear stiffness matrices as

$$[M]\{\ddot{W}\}_t + ([K] - [K_{N\Delta T}] + [K_r] + [N_1]_s + [N_2]_s)\{W\}_t + \left(\tfrac{1}{2}[N_1]_t + \tfrac{1}{3}[N_2]_t + [N_2]_{st}\right)\{W\}_t = 0 \quad (35)$$

Note that the sum of linear matrices is just the tangent stiffness $[K_{\tan}]$ in the Newton–Raphson iteration method. Equation (35) can solved as a standard eigenvalue problem to obtain the linear frequencies and mode shapes of a thermally buckled composite plate about the buckled equilibrium position $\{W\}_s$ by neglection of the nonlinear stiffness terms as

$$[M]\{\ddot{W}\}_t + [K_{\tan}(W_s)]\{W\}_t = 0 \quad (36)$$

where the converged tangent stiffness matrix at ΔT is

$$[K_{\tan}(W_s)] = [K] - [K_{N\Delta T}] + [K_r] + [N_1]_s + [N_2]_s \quad (37)$$

Examples and Discussion

A 15 × 12 × 0.05-in. (38.1 × 30.48 × 0.13-cm), eight-layered $[0/-45/45/90]_s$ graphite–epoxy rectangular plate with and without embedded SMA wires is studied in detail. SMA wires are embedded in all eight layers, and they are aligned in the same direction as the graphite fibers. The SMA austenite start temperature A_s of Nitinol is set to 70°F (21°C), so that the SMA phase transformation can be activated at the reference temperature. This can be achieved by adjustment of the nickel content[3] in Nitinol to 55.6%. A titanium plate is also studied for comparison. The material properties of graphite–epoxy are also considered TD, and titanium is considered TI. The material properties of Nitinol, graphite–epoxy composite, and titanium alloy are listed in Table 1. Because of symmetry, one-quarter of the plate is modeled with a 6 × 6 mesh or 36 Bogner–Fox–Schmit[25] rectangular elements. Both simply supported and clamped boundary conditions are considered. The in-plane support conditions are immovable because $u = 0$ at $x = 0$ and a; $v = 0$ at $y = 0$ and b, where a and b are the length and width of the plate, respectively.

Table 2 Critical buckling temperatures of plates

Plate		Simply supported, °F (°C)	Clamped, °F (°C)
Titanium		73.6 (23.1)	79.8 (26.6)
Graphite–epoxy			
$v_s = 0\%$	$\varepsilon_r = 0\%$	84.9 (29.4)	107.5 (41.9)
10%	3%	208.9 (98.3)	243.8 (117.7)
10%	5%	363.2 (184.0)	395.9 (202.2)
20%	3%	446.4 (230.2)	481.6 (249.8)

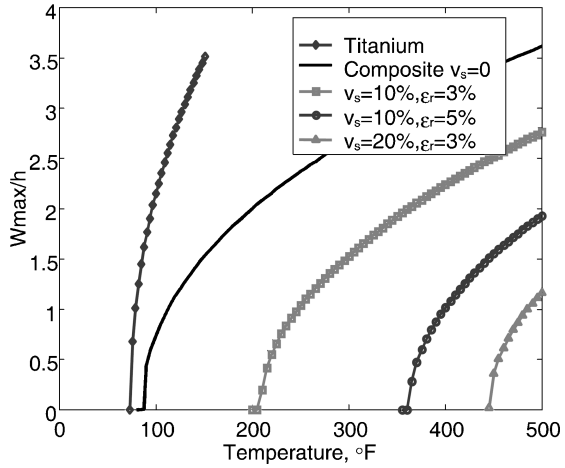

Fig. 3 Nondimensional maximum deflection of the simply supported plates.

Table 2 shows the critical temperatures for titanium and composite plates with or without SMA when the iterative eigenvalue scheme is used. It is demonstrated that SMA increases the critical temperature greatly for the graphite–epoxy composite plates. In other words, the recovery stress from the embedded SMA enlarges the desired buckling-free temperature range. Skin panels of QSP could reach 350°F at cruise. The results indicate that the clamped composite plates embedded with SMA ($v_s = 10\%$ and $\varepsilon_r = 5\%$) and ($v_s = 20\%$ and $\varepsilon_r = 3\%$) are both suitable for QSP application.

The postbuckling deflections of the titanium and composite plates with simply supported and clamped boundary conditions are calculated by the use of the Newton–Raphson method and are shown in Figs. 3 and 4, respectively. The indicated critical temperatures

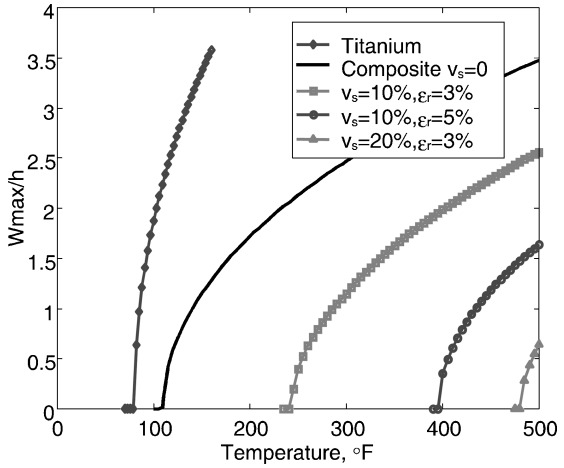

Fig. 4 Nondimensional maximum deflection of the clamped plates.

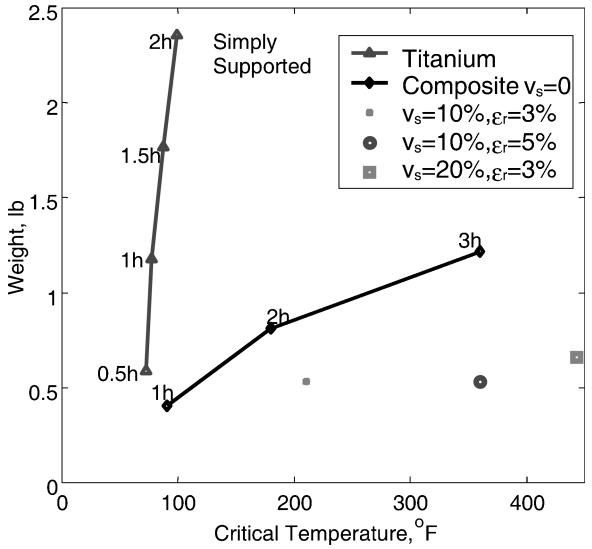

Fig. 5 Plate weight vs T_{cr} for simply supported plates (base h = 0.050 in.).

from Figs. 3 and 4 are the same as those obtained with the iterative eigenvalue scheme. It is obvious that the postbuckling deflections are much smaller for the SMA embedded composite plate than either the titanium or the traditional composite plate without SMA for a given temperature.

The mass density of graphite–epoxy is 1550 kg/m^3. Nitinol and titanium are much heavier. The savings in weight based on critical temperature are presented in Figs. 5 and 6 for the simply supported and the clamped cases, respectively. For titanium and traditional composite ($v_s = 0$) plates, the thickness of the plates is varied through a multiple of the base thickness $h = 0.05$ in. (1.25 mm). It is shown that to achieve a given T_{cr}, for example, 350°F (177°C), the weight of a simply supported plate with SMA ($v_s = 10\%$ and $\varepsilon_r = 5\%$) is about 0.53 lb (0.24 kg), whereas the weight is 1.2 lb (0.54 kg) for traditional composite plate of thickness $3h$ (0.15 in.). Obviously, the weight of the titanium plate is the heaviest and other means such as size reduction should be performed for the titanium plate to reach a critical temperature of 350°F.

The lowest three linear frequencies about the thermally buckled equilibrium position vs temperature for the traditional composite plate and the plate embedded with SMA ($v_s = 10\%$ and $\varepsilon_r = 5\%$) are shown in Figs. 7 and 8, respectively. At $T = T_{cr}$ the fundamental frequencies for both cases go to zero. In Fig. 7, the frequencies decrease between T_{ref} and T_{cr} due to the thermal expansion effect. At T_{cr}, the plate loses the static stability and the bifurcation deflection occurs. The frequencies increase after passing T_{cr} because the

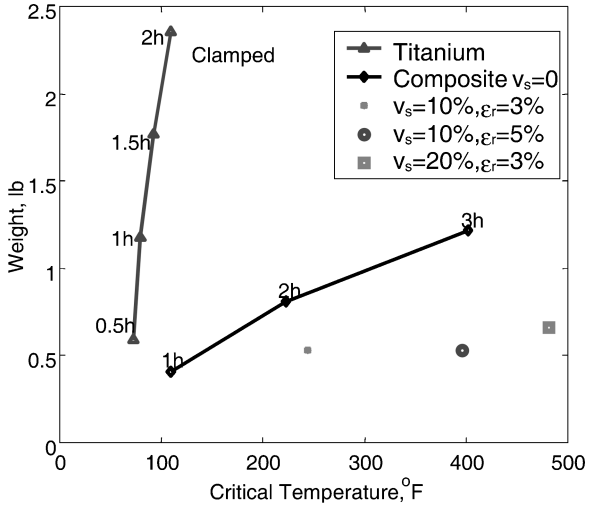

Fig. 6 Plate weight vs T_{cr} for clamped plates (base h = 0.050 in.).

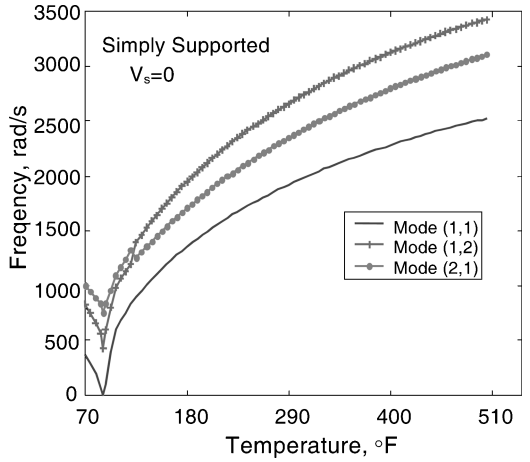

Fig. 7 Linear frequencies vs temperature for a simply supported composite plate without SMA.

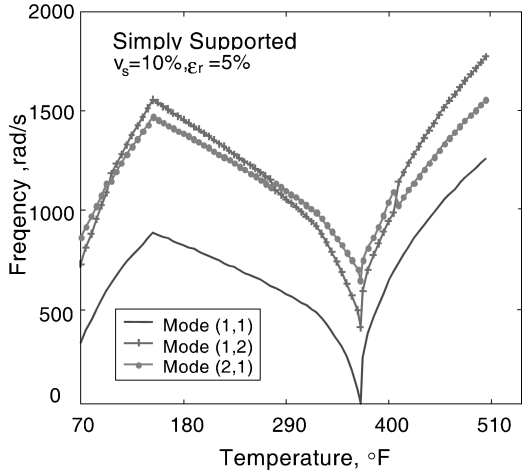

Fig. 8 Linear frequencies vs temperature for a simply supported composite plate with SMA (v_s = 10% and ε_r = 5%).

geometrical nonlinearity contributes stiffness to the plate. There is also a modal crossing at $T = 120$°F (49°C). In Fig. 8, the frequencies first increase, then decrease between T_{ref} and T_{cr}. This is due to the interaction between the SMA recovery stress and the thermal expansion effect. When the temperature is low, the SMA recovery stress overwhelms the thermal expansion effect and makes the plate stiffer. As the temperature increases further, the SMA recovery stress gradually becomes saturated, and the thermal expansion

effect gradually dominates. Clearly, the plate tends to be stiffer as temperature increases within a certain range due to the contribution of SMA recovery stress. Three modal crossings are also observed within the temperature range studied.

Conclusions

An efficient finite element formulation is presented for the determination of critical temperature, postbuckling, and vibration about the buckled equilibrium positions of SMA embedded composite plates. Nonlinear TD material properties of SMA and von Kármán large deflection are considered in the formulation. Examples show that the critical temperature of a composite plate embedded with SMA is successfully increased far beyond that of the traditional composite plate. Within the working temperature range of 350°F for QSP, the thermal buckling can be completely suppressed. It would cost a great deal in weight penalty for the traditional composite plate to achieve this same goal. Results demonstrated that it is feasible to suppress thermal deflections with proper percentages of SMA volume fraction and prestrain for QSP application. The thermal buckling study is the first step toward the use of SMA for supersonic vehicle applications. The consecutive parts that are currently under investigation include 1) the suppression of supersonic nonlinear panel flutter, and 2) the reduction of large-amplitude random response of surface panels when SMA is used. The results will be reported as soon they are prepared for disclosure.

References

[1]Wilson, J. R., "The New Shape of Supersonics," *Aerospace America*, Vol. 40, No. 6, 2002, pp. 26–33.

[2]Cheng, G., Mei, C., and Chen, R. R., "Methodology for Supersonic Panel Flutter Analysis of Thermal Protection System," *Journal Aircraft*, Vol. 38, No. 6, 2001, pp. 1025–1031.

[3]Buehler, W. J., and Wang, F. E., "A Summary of Recent Research on the Nitinol Alloys and Their Potential Applications in Ocean Engineering, *Ocean Engineering*, Vol. 1, No. 1, 1968, pp. 105–120.

[4]Cross, W. B., Kariotis, A. H., and Stimler, F. J., "Nitinol Characterization Study," NASA CR-1433, 1970.

[5]Saunders, W. R., Robertshaw, H. H., and Rogers, C. A., "Experiment Studies of Structural Acoustic Control for a Shape Memory Alloy Beam," *Proceedings of the 31st Structures, Structural Dynamics, and Materials Conference*, AIAA, Washington, DC, 1990, pp. 2274–2282.

[6]Turner, T. L., "Dynamic Response Tuning of Composite Beams by Embedded Shape Memory Alloy Actuators," *Proceedings of the Society of Photo-Optical Instrumentation Engineers 7th Symposium on Smart Structures and Materials*, SPIE Vol. 3991-47, International Society for Optical Engineering, Bellingham, WA, 2000.

[7]Turner, T. L., "Thermomechanical Response of Shape Memory Alloy Hybrid Composites," NASA TM-2001-210656, 2001.

[8]Birman, V., "Review of Mechanics of Shape Memory Alloy Structures," *Applied Mechanics Reviews*, Vol. 50, Pt. 1, No. 11, 1997, pp. 629–645.

[9]Thornton, E. A., "Thermal Buckling of Plates and Shells," *Applied Mechanics Reviews,* Vol. 46, No. 10, 1993, pp. 485–506.

[10]Noor, A. K., and Burton, W. S., "Computational Models for High-Temperature Multilayered Composite Plates and Shells," *Applied Mechanics Reviews,* Vol. 45, No. 10, 1992, pp. 419–446.

[11]Tauchert, T. R., "Thermally Induced Flexure, Buckling, and Vibration of Plates," *Applied Mechanics Reviews*, Vol. 44, No. 8, 1991, pp. 347–360.

[12]Kamiya, N., and Fukui, A., "Finite Deflection and Postbuckling Behavior of Heated Rectangular Plates with Temperature-Dependent Properties," *Nuclear Engineering and Design*, Vol. 72, No. 3, 1982, pp. 415–420.

[13]Chen, L. W., and Chen, L. Y., "Thermal Buckling Behavior of Laminated Composite Plates with Temperature-Dependent Properties," *Composite Structures*, Vol. 13, No. 4, 1989, pp. 275–287.

[14]Chen, L. W., and Chen, L. Y., "Thermal Postbuckling Behavior of Laminated Composite Plates with Temperature-Dependent Properties," *Composite Structures*, Vol. 19, No. 3, 1991, pp. 267–283.

[15]Noor, A. K., and Burton, W. S., "Three-Dimensional Solutions for the Thermal Buckling and Sensitivity Derivatives of Temperature-Sensitive Multilayered Angle-Ply Plates," *Journal of Applied Mechanics*, Vol. 59, No. 10, 1992, pp. 848–856.

[16]Lee, I., Oh, I. K., and Lee, D. M., "Vibration and Flutter Analysis of Stiffened Composite Plate Considering Thermal Effect," AD-Vol. 55, *Proceedings of the ASME Aerospace Division, International Mechanical Engineering Congress*, American Society of Mechanical Engineering, New York, 1997, pp. 133–141.

[17]Mei, C., Duan, B., and Zhong, Z. W., "Large Thermal Deflections of Composite Plates with Temperature Dependent Properties," U.S. Air Force Weapons Lab., AFWL-VA-WP-TR-1999-3036, Wright–Patterson AFB, OH, Feb. 1999.

[18]Duan, B., "Suppression of Composite Panel Vibration Under Combined Aerodynamic and Acoustic Excitations at Elevated Temperatures Using Shape Memory Alloy," Ph.D. Dissertation, Aerospace Engineering Dept., Old Dominion Univ., Norfolk, VA, May 2001.

[19]Duan, B., Tawfik, M., Goek, S. N., Ro, J. J., and Mei, C., "Analysis and Control of Large Thermal Deflection of Composite Plates Using Shape Memory Alloy," *Proceedings of the Society of Photo-Optical Instrumentation Engineers, 7th Annual International Symposium on Smart Structures and Materials*, SPIE Vol. 3991-45, International Society for Optical Engineering, Bellingham, WA, 2000.

[20]Tawfik, M., Ro, J.-J., and Mei, C., "Thermal Postbuckling and Aeroelastic Behavior of Shape Memory Alloy Reinforced Plates," *Smart Materials and Structures*, Vol. 11, No. 2, 2002, pp. 297–307.

[21]Lee, J. J., and Choi, S., "Thermal Buckling and Postbuckling Analysis of a Laminated Composite Beam with Embedded SMA Actuators,"*Composite Structures*, Vol. 47, No. 1–4, 1999, pp. 695–703.

[22]Lee, H. J., Lee, J. J., and Huh, J. S., "A Simulation Study on the Thermal Buckling Behavior of Laminated Composite Shells with Embedded Shape Memory Alloy (SMA) Wires," *Composite Structures*, Vol. 47, No. 1–4, 1999, pp. 463–469.

[23]Thompson, S. P., and Loughlan, J., "Enhancing the Postbuckling Response of a Composite Panel Structure Utilizing Shape Memory Alloy Actuators—A Smart Structural Concept," *Composite Structures*, Vol. 51, No. 1, 2001, pp. 21–36.

[24]Nowacki, W., *Thermoelasticity*, Addison Wesley, Longman, Reading, MA, 1962, Chap. IX.

[25]Bogner, F. K., Fox, R. L., and Schmit, L. A., "The Generation of Inter-Element Compatible Stiffness and Mass Matrices by the Use of Interpolation Formulas," U.S. Air Force Flight Dynamics Lab., AFFDL-TR-66-80, Wright–Patterson AFB, OH, 1966, pp. 396–443.